

1  
2  
3 1 CELLULAR EVENTS INVOLVED IN *E. coli* CELLS INACTIVATION BY  
4  
5 2 SEVERAL AGENTS FOR FOOD PRESERVATION: A COMPARATIVE  
6  
7 3 STUDY.  
8  
9  
10 4

11  
12 5 María Marcén, Guillermo Cebrián, Virginia Ruiz-Artiga, Santiago Condón and Pilar  
13  
14 6 Mañas\*

15  
16 7 **Running title:** Cellular events in treated *E. coli*  
17  
18 8

19  
20 9 Tecnología de los Alimentos, Facultad de Veterinaria de Zaragoza, Instituto  
21  
22 10 Agroalimentario de Aragón– IA2 - (Universidad de Zaragoza-CITA), Zaragoza, Spain  
23  
24 11

25  
26  
27 12 \*Corresponding author: Pilar Mañas

28  
29 13 Postal address: Tecnología de los Alimentos, Facultad de Veterinaria, C/ Miguel Servet,  
30  
31 14 177, 50013, Zaragoza, Spain.

32  
33 15 Tel No.: +34876554136  
34

35 16 E-mail: manas@unizar.es  
36  
37 17  
38  
39  
40  
41  
42  
43  
44  
45  
46  
47  
48  
49  
50  
51  
52  
53  
54  
55  
56  
57  
58  
59

60  
61  
62 **18 ABSTRACT**  
63

64 19 Traditional and novel technologies for food preservation are being investigated to obtain  
65 20 safer products and fulfil consumer demands for less processed foods. These  
66 21 technologies inactivate microorganisms present in foods through their action on  
67 22 different cellular targets, but the final cause of cell loss of viability often remains not  
68 23 well characterized. The main objective of this work was to study and compare cellular  
69 24 events that could play a role on *E. coli* inactivation upon exposure to treatments with  
70 25 technologies of different nature. *E. coli* cells were exposed to heat, high hydrostatic  
71 26 pressure (HHP), pulsed electric fields (PEF) and acid treatments, and the occurrence of  
72 27 several alterations, including presence of sublethal injury, membrane permeabilization,  
73 28 increased levels of reactive oxygen species (ROS), DNA damage and protein damage  
74 29 were studied. Results reflected differences among the relevance of the several cellular  
75 30 events depending on the agent applied. Sublethally injured cells appeared after all the  
76 31 treatments. Cells consistently recovered in a higher percentage in non-selective medium,  
77 32 particularly in minimal medium, as compared to selective medium; however this effect  
78 33 was less relevant in PEF-treated cells. Increased levels of ROS were detected inside  
79 34 cells after all the treatments, although their order of appearance and relationship with  
80 35 membrane permeabilization varied depending on the technology. A high degree of  
81 36 membrane permeabilization was observed in PEF treated cells, DNA damage appeared  
82 37 as an important target in acid treatment, and protein damage, in HHP treated cells.  
83 38 Results obtained help to understand the mode of action of food preservation  
84 39 technologies on bacterial cells.

85 40 **KEYWORDS:** heat, acid, PEF, HHP, sublethal injury, cellular alterations.  
86 41  
87 42

119  
120  
121 **43 1. INTRODUCTION**  
122

123 44 Food preservation is a continuous fight against pathogenic and spoilage  
124  
125 45 microorganisms in order to obtain safe products. However, consumers not only  
126  
127  
128 46 expect safe products, but also demand products which keep their nutritional and  
129  
130 47 sensorial properties. With the purpose of achieving consumer demands, the food  
131  
132 48 industry investigates novel technologies for food preservation. Some of the most  
133  
134 49 investigated technologies are non-thermal technologies such as high hydrostatic  
135  
136 50 pressure (HHP) and pulsed electric fields (PEF). Besides, optimization of traditional  
137  
138 51 techniques such as heat treatments, acidity, natural antimicrobials, packaging  
139  
140 52 systems, etc., continues to be an important research topic. To obtain a better profit  
141  
142  
143 53 of all these technologies and to design appropriate combined processes, it is necessary  
144  
145 54 to gain deeper insight into their mode of action on microorganism.

146  
147 55 Within a bacterial cell, there are many potential cellular targets that may be affected  
148  
149 56 by a given stressing agent; some of them are considered as critical targets, whereas  
150  
151 57 others are not essential for bacterial survival (Miles, 2006). In addition, there are  
152  
153 58 tight interrelationships between the various structures and cellular functions; therefore,  
154  
155 59 the alteration of a particular structure or function may indirectly affect another one  
156  
157 60 (Mackey and Mañas, 2008). Furthermore, the degree of damage exerted to the  
158  
159 61 different cellular targets is also an important factor, since damages in critical  
160  
161 62 components at low intensity may produce sublethal injury; similarly, damages in non-  
162  
163 63 critical components may also render sublethally injured cells. These cells can repair  
164  
165 64 their damages and resume growth only if the environmental conditions are  
166  
167 65 appropriate (Mackey, 2000). In summary, identifying the particular structures and  
168  
169 66 processes whose alteration leads to cell death is a difficult task.

170  
171  
172 67 Nowadays, it is generally accepted that heat treatment has a multi-target mode of  
173  
174  
175  
176  
177

178  
179  
180 68 action on microorganisms, since it is able to cause alterations at different cellular  
181  
182 69 levels. These include cytoplasmic membrane damage, outer membrane damage, DNA  
183  
184 70 strand breaks, inactivation of enzymes, protein coagulation, etc (Lado and Yourself,  
185  
186 71 2002; Mackey, 2000). HHP is also considered a multi-target technology, affecting  
187  
188 72 envelopes integrity, DNA and protein conformation, ribosomes configuration etc.  
189  
190 73 (Aertsen et al., 2005; Mackey and Mañas, 2008; San Martín et al., 2002). Studies about  
191  
192 74 PEF have described that electroporation in the cytoplasmic membrane is the main  
193  
194 75 cellular alteration during exposure to this technology (Mañas and Pagán, 2005). On  
195  
196 76 the other hand, although much less information is available, envelopes, protein and  
197  
198 77 DNA damage are considered as important targets to inactivate microorganisms by acid  
199  
200 78 pH (Richard and Foster, 2004; Van de Guchte et al., 2002). Despite the different mode  
201  
202 79 of action of the various technologies, the cytoplasmic membrane appears as a common  
203  
204 80 target in most cases.

205  
206  
207 81 It is important to note that, despite these general observations about the different  
208  
209 82 technologies are generally assumed, the precise mode of action on bacterial cells, and  
210  
211 83 the relative importance of the various cellular alterations on cell survival or inactivation  
212  
213 84 remains largely understudied. Currently, a new aspect is gaining importance as a  
214  
215 85 possible common mechanism of microbial inactivation of all of these technologies: the  
216  
217 86 oxidative component (Mols and Abee, 2011). There are scattered reports of increased  
218  
219 87 ROS levels in cells treated by physical and chemical agents. In this way, it has been  
220  
221 88 proven that higher levels of ROS are detected in heat treated *E. coli* cells (Baatout et al.,  
222  
223 89 2005; Marcén et al., 2017). Besides, some authors demonstrated that HHP treatment  
224  
225 90 induces cytoplasmic oxidative stress in *E. coli* (Aertsen et al., 2005; Malone et al.,  
226  
227 91 2006). Pakhomova et al. (2012) suggested that in PEF treatment (nanosecond  
228  
229 92 pulses) the increase in non-selective transmembrane cation conductance may be in  
230  
231  
232  
233  
234  
235  
236

237  
238  
239 93 part mediated by oxidative stress, and ROS formation could be a factor contributing to  
240  
241 94 the cytotoxic effects in eukaryotic cells. Finally, Mols et al. (2010) supported the idea  
242  
243 95 that acid stress also induced oxidative stress. These authors proposed that the formation  
244  
245 96 of radicals such as OH<sup>-</sup> may be a common mechanism of cellular death when  
246  
247 97 bacteria are exposed to different stress conditions. Increased ROS levels have been  
248  
249 98 attributed to disturbances in the electron transport as a consequence of alterations in  
250  
251 99 cytoplasmic membrane integrity and functionality. However, levels of ROS within  
252  
253 100 bacterial cells may also increase depending on other factors such as the loss of activity  
254  
255 101 of scavenging enzymes, the loss of antioxidant molecules, or the presence of free  
256  
257 102 iron in the cytoplasm, among other factors (De Spiegeleer et al., 2004; Gusarov and  
258  
259 103 Nudler, 2005; Imlay, 2013).

262  
263 104 This research was aimed to obtain robust and systematic data in order to clarify the  
264  
265 105 main cellular events involved in the inactivation of bacteria by food preservation  
266  
267 106 technologies of different nature and the possible relationship between them. To reach  
268  
269 107 this objective, the presence of ROS and the permeabilization of the membrane after  
270  
271 108 heat, HHP, PEF and acid treatments was determined and comparisons among the  
272  
273 109 different agents were made. Moreover, other cellular alterations that could be involved  
274  
275 110 in cell inactivation were also studied in order to gain knowledge about the mode of  
276  
277 111 action of these stressing agents on bacteria.

## 279 112 **2. MATERIAL AND METHODS**

### 282 113 *2.1. Bacterial strains and growth conditions*

284 114 *Escherichia coli* BW25113 and its isogenic mutants JW0013 ( $\Delta$ DnaK:kan) and,  
285  
286 115 JW2669 ( $\Delta$ RecA:kan) were used in this study. The strains were stored at -80°C. To  
287  
288 116 prepare preculture, a flask containing 10 mL of sterile TSBYE (Tryptic Soy Broth  
289  
290 117 with 0.6% Yeast Extract, Oxoid, Basingstoke, UK) was inoculated with one single

296  
297  
298 118 colony from a TSAYE plate (Tryptic Soy Agar with 0.6 % Yeast Extract, Oxoid) for  
299  
300 119 parental strain, and a TSAYE plus kanamycin (0.05 mg/mL) plate for mutant strains.  
301  
302 120 The preculture was incubated overnight at 37°C, under agitation. Subsequently, a  
303  
304 121 culture was obtained by inoculating a flask with 50 mL TSBYE with 100 µL of the  
305  
306 122 preculture, and incubating under agitation at 37°C for 18-24 hours until stationary  
307  
308 123 phase of growth ( $1-2 \times 10^9$  CFU/ mL, approximately).  
309  
310

### 311 124 *2.2. Heat treatment*

312  
313 125 Heat treatments were carried out in glass tubes, which contained 4.5 mL of sterile PBS  
314  
315 126 (Phosphate Buffered Saline, Sigma, San Louis, Missouri, USA) as treatment medium,  
316  
317 127 submerged and prewarmed at 58°C in a thermostated water bath. Five hundred µL of  
318  
319 128 the bacterial culture was inoculated to reach an initial concentration of  $10^8$  CFU/ mL,  
320  
321 129 approximately, and after different heating times, samples were collected, immediately  
322  
323 130 cooled and kept for further analysis.  
324  
325

### 326 131 *2.3. High hydrostatic pressure treatments*

327  
328 132 Stansted Fluid Power S-FL-085-09-W (Harlow, London, England) equipment was  
329  
330 133 used to carry out HHP treatments (Ramos et al., 2015). A mixture of propylene glycol  
331  
332 134 and distilled water (50/50, v/v) was used as the pressure transmitting fluid. An  
333  
334 135 automatic device was employed to set and/or record the pressure, time and temperature  
335  
336 136 during the pressurization cycle. Cell suspensions were centrifuged and diluted to a cell  
337  
338 137 concentration of  $10^8$  CFU/ mL in PBS, approximately. Samples were packed in plastic  
339  
340 138 bags, which were sealed and introduced in the equipment treatment chamber.  
341  
342 139 Treatments were applied at 300 MPa during different treatment times up to 30 min,  
343  
344 140 and temperature never exceeded 40°C.  
345  
346

### 347 141 *2.4. Pulsed electric field treatment*

355  
356  
357 142 PEF equipment used in this investigation was supplied by ScandiNova (Modulator PG,  
358  
359 143 ScandiNova, Uppsala, Sweden). The equipment and treatment chamber used in this  
360  
361 144 investigation were previously described by Saldaña et al. (2010). For PEF treatments,  
362  
363 145 cells were dissolved in McIlvaine buffer, which allowed a simultaneous adjustment of  
364  
365 146 pH (7.0) and conductivity (1 mS/cm), at a concentration of  $10^8$  CFU/ mL. Samples  
366  
367 147 were introduced in the treatment chamber of the PEF equipment, which had a gap of  
368  
369 148 0.25 cm. A square pulse with a width of 3  $\mu$ s, a frequency of 0.5 Hz (1 pulse per 2  
370  
371 149 seconds), electric field strength of 20 kV/cm and  $<40^\circ\text{C}$  of temperature were used  
372  
373 150 during the treatment. Under these experimental conditions, the energy per pulse was  
374  
375 151 1.20 kJ/kg. Treatments of up to 100 pulses (300  $\mu$ s) were applied.  
376  
377

### 378 152 2.5. Acidity treatment

379  
380 153 TSBYE was acidified to pH 3.0 with lactic acid and then filter-sterilized. Cells were  
381  
382 154 added to a concentration of  $10^8$  CFU/ mL, and temperature was kept constant at  $25^\circ\text{C}$ .  
383  
384 155 One hundred  $\mu\text{L}$  samples were withdrawn at intervals, up to 120 min, and transferred  
385  
386 156 into 900  $\mu\text{L}$  of TSBYE for neutralization (Cebrián et al., 2010).  
387  
388 157 The treatment parameters for heat, HHP, PEF and acidity (intensity and exposure  
389  
390 158 times) were chosen from preliminary experiments (data not shown), in order to achieve  
391  
392 159 a slow *E. coli* inactivation, to study damages in different cellular targets under  
393  
394 160 equivalent lethality conditions for the four agents.  
395  
396

### 397 161 2.6. Recovery after treatments and survival curves

398  
399 162 After each treatment, samples were serially diluted in MRD (Maximum Recovery  
400  
401 163 Diluent, Oxoid) and pour-plated in TSAYE for survival counts. Plates were incubated  
402  
403 164 at  $37^\circ\text{C}$  in aerobic conditions and after 24-72 h CFU were counted. With the purpose of  
404  
405 165 constructing survival curves, the fraction of survivors ( $\text{Log } N_t/N_0$ ) was represented vs the  
406  
407 166 treatment time (min for heat, HHP and acid treatments, and  $\mu$ s in PEF treatment). Under  
408  
409  
410  
411  
412  
413

414  
 415  
 416 167 most experimental conditions deviations from linearity were observed, and therefore the  
 417  
 418 168 Geeraerd inactivation model-fitting tool (GInaFiT) (Geeraerd et al., 2005) was used to fit  
 419  
 420 169 survival curves and to calculate resistance parameters. As survival curves obtained in this  
 421  
 422  
 423 170 investigation generally showed shoulders, the log linear regression plus shoulder model  
 424  
 425 171 was used in the majority of the experiments (Equation 1). However, in the particular case  
 426  
 427 172 of PEF treatments, survival curves showed a linear portion plus a tail, so in this case the  
 428  
 429 173 log linear regression plus tail was used (Equation 2) (Geeraerd et al., 2000).

431  
 432 174 
$$N(t) = N(0) \cdot e^{-k_{max} \cdot t} \cdot \left[ \frac{e^{k_{max} \cdot S_l}}{1 + (e^{k_{max} \cdot S_l} - 1) \cdot e^{-k_{max} \cdot t}} \right] \quad (1)$$

433  
 434  
 435 175 
$$N(t) = (N(0) - N_{res}) \cdot e^{-k_{max} \cdot t} + N_{res} \quad (2)$$

436  
 437 176 In these equations  $N(t)$  represents the number of survivors,  $N(0)$  the initial count and  $t$   
 438  
 439 177 the time for treatments. Furthermore, to describe the survival curves, these two models  
 440  
 441 178 use the following parameters: shoulder length ( $S_l$ ), defined as the time before the  
 442  
 443 179 exponential inactivation begins; inactivation rate ( $k_{max}$ ), defined as the slope of the  
 444  
 445 180 exponential portion of the survival curve; and  $N_{res}$  which describes the residual  
 446  
 447 181 population density (tail).

448  
 449  
 450 182 The traditional decimal reduction time value ( $D$ ) of each survival curve was calculated  
 451  
 452 183 from  $k_{max}$  (Equation 3).

453  
 454 184 
$$D = 2.303/k_{max} \quad (3)$$

455  
 456 185  $2D$  values were also calculated. In this case  $2D$  is defined as the dose necessary to  
 457  
 458 186 inactivate 2 Log<sub>10</sub>-cycles of the initial population, and is calculated by Equation 4.

459  
 460 187 
$$2D = S_l + 2 \times D \quad (4)$$

461  
 462 188 Where  $S_l$  is the shoulder length duration and  $D$  is the inactivation parameter calculated  
 463  
 464 189 from Equation 3.

465  
 466  
 467 190 Where indicated in the text, cells were also recovered in minimal M9 glucose-salts agar  
 468  
 469  
 470  
 471  
 472



473  
474  
475 191 enriched with 3 mM L-cysteine HCl (MM-cys) (Sigma Aldrich, Milan, Italy) under  
476  
477 192 anaerobic atmosphere (MACS VA500 Microaerophilic Workstation, DW Scientific, UK).  
478  
479 193 M9 agar was prepared as described previously (Gerhardt et al., 1994), supplemented with  
480  
481 194 FeSO<sub>4</sub> (10 mg/L) to improve bacterial growth (Stanier et al., 1992), and with cysteine to  
482  
483 195 create a low redox potential medium (Gerhardt et al., 1994; Suh and Knabel, 2000). On  
484  
485 196 the other hand, a selective medium which consisted of TSAYE with the maximum non  
486  
487 197 inhibitory concentration of NaCl (4%) determined in previous experiments (data not  
488  
489 198 shown) (Panreac S.A, Barcelona, Spain), was used to detect the number of sublethally  
490  
491 199 damaged cells (Mackey, 2000). In order to quantify and compare the proportion of  
492  
493 200 sublethally damaged cells appearing after exposing cells to the different agents, the area  
494  
495 201 under the curve (time units × Log N<sub>t</sub>/N<sub>0</sub>) was calculated with the GraphPad PRISM 5  
496  
497 202 software (GraphPad Software, Inc., San Diego, CA, USA) as described by Lou and  
498  
499 203 Yousef (1997), fixing a treatment time corresponding to 2 Log cycles of inactivation  
500  
501 204 under standard recovery conditions (TSAYE). The population displaying sublethal  
502  
503 205 damage corresponds to the area under the curve of cells recovered in selective medium,  
504  
505 206 minus the area under the curve of cells recovered in non-selective one for a fixed  
506  
507 207 exposure time. Since survival curves corresponding to the different technologies were  
508  
509 208 not directly comparable because of their different treatment lengths; the ratio between  
510  
511 209 both areas was calculated, instead of the difference, in order to establish meaningful  
512  
513 210 comparisons.

### 2.7. ROS and membrane permeabilization determinations

518 211 The presence of ROS and membrane permeabilization in cells after exposure to the  
519  
520 212 treatments was studied through staining with specific fluorochromes followed by  
521  
522 213 epifluorescence microscopy. Treated cells were collected and stained separately with  
523  
524 214 DHE (dihydroethidium) (Life Technologies), HPF (hydroxyphenyl fluorescein) (Sigma  
525  
526 215

532  
533  
534 216 Aldrich) and PI (propidium iodide) (Sigma Aldrich). In some experiments, where  
535  
536 217 indicated in the text, double staining was performed, by the use of two dyes combined  
537  
538 218 simultaneously. The combinations used were DHE plus HPF, and HPF plus PI. Treated  
539  
540 219 cells were incubated with the fluorescent dye at a cell concentration of approximately  $10^8$   
541  
542 220 CFU/mL, then centrifuged and resuspended in PBS. A positive and a negative control  
543  
544 221 were always included. Staining conditions were 50  $\mu$ M/90 min for DHE and HPF and 3  
545  
546 222  $\mu$ M/30 min for PI (Klotz et al. 2010; Marcén et al., 2017; Mols et al., 2009; Patsoukis et  
547  
548 223 al., 2005). The results obtained were analyzed by phase contrast and fluorescence  
549  
550 224 microscopy (Nikon Eclipse E400, Nikon Corporation, Japan), in order to obtain the  
551  
552 225 percentage of stained cells. Images were obtained with a high resolution camera  
553  
554 226 (AxioCam MRc, Zeiss, Germany) and processed with the software ZEN 2012 (Zeiss,  
555  
556 227 Germany). Total and fluorescent cells were counted from photographs taken from each  
557  
558 228 sample, and at least three different representative microscopic fields, containing 100-200  
559  
560 229 cells, approximately, were used for quantification.

#### 563 230 2.8. Measurement of DNA damage by qualitative PCR assays.

564 231 Bacterial DNA damage was measured semi quantitatively following the fundamentals of  
565  
566 232 the method reported by Park and Imlay (2003), based on the fact that damaged DNA  
567  
568 233 renders a less effective amplification with a high fidelity polymerase. Total genomic  
569  
570 234 DNA, either from untreated or from treated cells, was isolated from 1 mL of culture using  
571  
572 235 a genomic DNA extraction kit (Realpure, Real Laboratory, Valencia, Spain). DNA was  
573  
574 236 quantified spectrophotometrically and diluted in MilliQ water to 10 ng/ $\mu$ L (Simplinano,  
575  
576 237 Biochrom, Cambridge, UK). A 1860 pb fragment upstream and downstream *rpoS* gene  
577  
578 238 was used for amplification. Primer sequences were as follows: 5'-  
579  
580 239 ACTGTCAGCAGTACATCAACCAGTA (forward primer) and 5'-  
581  
582 240 GTTACCAGCCGCATTTATTATTTC (reverse primer). The 20  $\mu$ L PCR mixture  
583  
584  
585  
586  
587  
588  
589  
590

591  
592  
593 241 contained 20 ng of genomic DNA as a template, a 40  $\mu\text{M}$  concentration (each) of the two  
594  
595 242 primers, 20 mM of the deoxynucleotide mix (Sigma), 5X Phusion HF Buffer and 1  $\mu\text{L}$  of  
596  
597 243 Phusion DNA Polymerase 2 U/ $\mu\text{L}$  (Thermo Scientific, Massachusetts, USA). Thermal  
598  
599 244 cycling was performed with a MultiGene II Personal Thermal Cycler (Labnet Biotecnica,  
600  
601 245 Madrid, Spain). The genomic DNA was initially denatured for 3 min at 98°C, and then  
602  
603 246 the DNA was subjected to 30 cycles of PCR, with 1 cycle consisting of denaturation at  
604  
605 247 98°C for 10 s and annealing at 66°C for 30 s and extension at 72°C for 90 s. A final  
606  
607 248 extension step at 72°C was performed for 10 min at the completion of the profile. PCR  
608  
609 249 products were separated by 1% agarose gel electrophoresis, stained with SYBR safe DNA  
610  
611 250 gel stain (Invitrogen, Carlsbad, CA, USA) and photographs were obtained with Gel Doc  
612  
613 251 XR (Bio-Rad Laboratories, Hercules, CA, USA).

### 614 252 *2.9. Statistical analysis*

615  
616  
617 253 All the experimental determinations were performed at least in triplicate with  
618  
619 254 independent microbial cultures, and data in **Figures** correspond to the average and the  
620  
621 255 mean standard deviation (error bars). **Survival curve fitting was carried out individually**  
622  
623 256 **for each replicate, resistance parameters obtained ( $S_b$ ,  $k_{max}$ ,  $N_{res}$ ,  $D$ ,  $2D$ ) and included in**  
624  
625 257 **Table 1 as the average and the mean standard deviation. Fitting performance was**  
626  
627 258 **indicated by the parameters RMSE (root mean squared error) and  $R^2$ .** Student's  $t$  tests  
628  
629 259 were carried out using the GraphPad PRISM 5 software (GraphPad Software, Inc., San  
630  
631 260 Diego, CA, USA), and differences were considered significant for  $p \leq 0.05$ .

## 632 261 **3. RESULTS AND DISCUSSION**

### 633 262 **3.1. Survival of *E. coli* to heat, HHP, PEF and acid.**

634  
635  
636 263 The resistance of *E. coli* cells to different agents was evaluated. In this way, cells were  
637  
638 264 treated by heat (58°C), HHP (300 MPa), PEF (20 kV/cm), and lactic acid (pH 3.0).  
639  
640 265 Figure 1 shows the survival curves of *E. coli* to the four technologies, obtained in  
641  
642  
643  
644  
645  
646  
647  
648  
649

650  
651  
652 266 TSAYE, TSAYE-NaCl and MM-Cys. The level of inactivation of *E. coli* cells to  
653  
654 267 heat, HHP, PEF, and lactic acid obtained was similar to that reported by other  
655  
656 268 authors, using a complex nutritional medium for the recovery of cells (Aertsen et al.,  
657  
658 269 2005; Álvarez et al., 2003; Benito et al., 1999; Cebrián et al., 2007). Experimental data  
659  
660 270 were fitted to the Geeraerd equation, and the parameters obtained are included in Table  
661  
662  
663 271 1. All the survival curves were adequately described by the Geeraerd equations  
664  
665 272 ( $R^2 \geq 0.97$ ), except the curve corresponding to acid treatment and MM-cys as recovery  
666  
667 273 medium, due to the insufficient inactivation attained after the longest exposure time  
668  
669 274 tested. As it can be observed in the graphs, the shape of the survival curves depended  
670  
671 275 on the agent applied. Convex or close to straight curves were obtained for heat, HHP  
672  
673 276 and acid treatments, whereas for PEF treatment the profile of the survival curves was  
674  
675 277 concave. For this reason, curves were fitted to the shoulder log-linear Geeraerd,  
676  
677 278 except those corresponding to PEF treatments, which needed the log-linear Geeraerd  
678  
679 279 equation provided with the mathematical adjustment to describe the tail portion. In this  
680  
681 280 study, tails appeared at an inactivation level of 3 Log cycles, approximately. The  
682  
683 281 presence of tails in PEF survival curves has been frequently reported and has been  
684  
685 282 associated to different phenomena, such as the presence of cells in the population with  
686  
687 283 different resistance to the treatment, adaptation phenomena along the treatment time or  
688  
689 284 heterogeneity within the treatment chamber. In contrast, convex curves are often  
690  
691 285 associated with the presence of a shoulder phenomenon, which has been attributed to  
692  
693 286 the occurrence of sublethally injured cells within the treated population (Cebrián et al.,  
694  
695 287 2007; Lou and Yourself, 1997; Mackey, 2000; Mañas and Pagán, 2005). To this regard,  
696  
697 288 the occurrence of an injured population is frequently estimated by the difference  
698  
699 289 between the number of viable cells in non selective medium (TSAYE) and in selective  
700  
701 290 medium, and normally the loss of the ability to grow in a selective medium with  
702  
703  
704  
705  
706  
707  
708

709  
710  
711 291 sodium chloride (TSAYE-NaCl) is interpreted as the loss of functionality of the  
712  
713 292 cytoplasmic membrane (Mackey, 2000; Wuytack et al., 2003). In this research we also  
714  
715 293 used minimum salts-glucose media with cysteine (MM-cys) under anaerobic  
716  
717 294 conditions to improve cells recovery. As Figure 1 shows, the four technologies here  
718  
719 295 studied lead to the appearance of sublethally damaged cells. For the four agents,  
720  
721 296 statistically significant differences ( $p<0.05$ ) were found among 2D values obtained for  
722  
723 297 the three different recovery conditions, and these differences were highly significant  
724  
725 298 (\*\*\*) for heat, HHP and acidity.

726  
727 299 According to our results, the relevance of sublethal damage seemed to be lower in  
728  
729 300 PEF-treated cells than in the other three technologies, since survival curves obtained  
730  
731 301 under the three recovery conditions used were closer in the case of PEF treatment,  
732  
733 302 which, in addition, showed absence of shoulder phenomena. The parameter area under  
734  
735 303 the curve (AUC, Table 1) offers an overall indication of the relative inactivation  
736  
737 304 provided by each treatment, therefore meaningful comparisons among recovery  
738  
739 305 conditions can be made. The ratios between the areas associated to the survival  
740  
741 306 curves obtained in TSAYE and in TSAYE- NaCl for heat, HHP, PEF and acid  
742  
743 307 treatments were 2.8, 2.2, 1.5 and 4.5, respectively (calculated from values in Table 1). As a  
744  
745 308 whole, these results would indicate that in PEF treated cells, and under the  
746  
747 309 experimental conditions here used, damage to the cytoplasmic membrane would be  
748  
749 310 more difficult to repair, and thus, probably more directly related to cell inactivation.

750  
751 311 Conversely, when cells were recovered in minimal medium MM-cys and anaerobic  
752  
753 312 atmosphere, the amount of survivors was higher for the four technologies studied (Fig  
754  
755 313 1, Table 1). Thus, these later conditions can be considered as more adequate for cell  
756  
757 314 repair after all the treatments applied. It has to be noted that anaerobic atmosphere  
758  
759 315 was not the only factor that favored cell recovery, since the number of survivors  
760  
761  
762  
763  
764  
765  
766  
767

768  
769  
770 316 obtained in TSAYE and anaerobiosis was very similar to that obtained under aerobic  
771  
772 317 recovery (data not shown). Also in this case, the ratios between the areas associated to  
773  
774 318 survival curves obtained in MM-cys and in TSAYE (3.0, 3.6, and 1.9 for heat, HHP  
775  
776 319 and PEF respectively) **confirmed** that for PEF treatments, the amount of cells with  
777  
778 320 sublethal injuries, able of recover and resume growth, was always lower. With regards  
779  
780 321 to the higher cell recovery observed in minimal medium MM-cys and anaerobic  
781  
782 322 atmosphere, it is reasonable to think that the protective effect observed in MM-cys  
783  
784 323 medium could be ascribed to its low redox potential and to the absence of oxidative  
785  
786 324 species generated during autoclaving, as previously demonstrated by other authors  
787  
788 325 (Mackey, 2000). These observations suggested that an oxidative component was  
789  
790 326 involved in cell inactivation and/or recovery after treatment, for the four technologies  
791  
792 327 here studied. It is important to keep in mind that, according to recovery data, also  
793  
794 328 cytoplasmic membrane alterations seemed to occur in cells treated by the four agents.  
795  
796  
797

798 329 **3.2. Exposure of *E. coli* cells to different technologies caused increase of ROS**  
799  
800 330 **levels and membrane permeabilization.**

801  
802 331 Treated cells were stained with different dyes to evaluate ROS presence. DHE  
803  
804 332 (dihydroethidium) was used for the detection of  $O_2^{\cdot-}$  due to its relative specificity for  
805  
806 333 this radical. Superoxide oxidizes the dye producing oxyethidium, which binds to DNA  
807  
808 334 showing strong red fluorescence (Gomes et al., 2005), although other reactive species  
809  
810 335 can also react with DHE (Zielonka and Kalyanaraman, 2010). We also used HPF 3'-(p-  
811  
812 336 hydroxyphenyl-fluorescein) which is oxidized by hydroxyl radicals producing green  
813  
814 337 fluorescence (Gomes et al., 2005). On the other hand, propidium iodide was used to  
815  
816 338 detect membrane permeabilization after treatment. This dye is not permeable, thus  
817  
818 339 it does not penetrate the cell unless the membrane is damaged. Once inside, it binds  
819  
820 340 to DNA and RNA and produces red fluorescence.  
821  
822  
823  
824  
825  
826

827  
828  
829 341 Figure 2 shows the percentage of stained and inactivated cells along time for each  
830  
831 342 treatment. It has to be noted that the inactivation is represented in a linear scale to  
832  
833 343 allow comparisons with the amount of stained cells. Treatments were applied in order  
834  
835 344 to obtain up to 90-99% of inactivation under standard recovery conditions (TSAYE,  
836  
837 **aerobiosis**) to enable comparisons among different treatments. Results showed that there  
838  
839 345 was an increase in ROS level and membrane permeabilization in *E. coli* cells upon exposure  
840  
841 346 to the four agents. The kinetics and order of appearance of both phenomena differed among  
842  
843 347 the technologies.  
844  
845 348  
846 349 Inactivation of heat treated cells proceeded progressively as the treatment time increased,  
847  
848 350 following a profile similar to the acquisition of DHE staining (Fig 2A). Staining with HPF  
849  
850 351 occurred later in time. The last phenomenon to happen was permanent permeabilization to  
852  
853 352 PI. For instance, after 2 **min** of exposure to 58°C, only 20% of the cells were permeable to  
854  
855 353 PI, whereas 90% of the cells were stained with DHE and also 90% were inactivated,  
856  
857 354 approximately. Under these treatment conditions, 70% of the cells, approximately,  
858  
859 355 presented staining with HPF. The response of *E. coli* to HHP treatments (Fig 2B) was  
860  
861 356 similar, although in this case DHE staining was faster and slightly above cell inactivation, in  
862  
863 357 the first **min** of treatment. Also in this case the percentage of cells permeabilized to PI  
864  
865 358 remained always lower than the percentage of inactivated cells.  
866  
867 359 For PEF treated cells (Fig 2C) close percentages of cell inactivation, membrane  
868  
869 360 permeabilization to PI and DHE staining were observed, whereas HPF staining took place  
870  
871 361 in a lower percentage of cells. Finally, acid-treated cells (Fig 2D) presented a high  
872  
873 362 percentage of staining with HPF and DHE, which was higher than that of inactivated cells.  
874  
875 363 The percentage of permeabilization to PI remained always below 30%, even when 90% of  
876  
877 364 cells appeared to be inactivated.  
878  
879  
880 365 Thus, results obtained in this study revealed that the kinetics and order of appearance  
881  
882  
883  
884  
885

886  
887  
888 366 of oxidative species and membrane permeabilization differed among the technologies.  
889  
890 367 Membrane permeabilization to PI seemed to occur simultaneously to cell inactivation  
891  
892 368 only in PEF treated cells, whereas in the other three technologies, a large percentage  
893  
894 369 of inactivated cells maintained a non permeable membrane to PI. Thus, inactivation  
895  
896 370 by heat, HHP and acidity seems to require additional cellular events other than loss  
897  
898 371 of permeability to PI of the cytoplasmic membrane. Although we cannot discard that  
899  
900 372 more subtle membrane alterations, that may contribute to cell inactivation, occurred in  
901  
902 373 these cells before permanent permeabilization to PI takes place, it seems clear from  
903  
904 374 our data that the degree of membrane alteration and its relevance in cell survival is  
905  
906 375 different depending on the technology applied. The results here obtained confirm the  
907  
908 376 pivotal role of the cytoplasmic membrane in cell inactivation by PEF, in comparison to  
909  
910 377 other agents. It is noteworthy, according to our results, that the use of the so-called  
911  
912 378 vital dyes to estimate bacterial viability requires a careful interpretation, since the  
913  
914 379 response to PI of *E. coli* seems to depend on the agent applied.  
915  
916  
917 380 On the other hand, also the order of appearance of the different ROS seemed to vary  
918  
919 381 depending on the treatment applied. For heat, HHP and PEF treatments, the amount of  
920  
921 382 cells stained with HPF was lower than the amount of cells stained with DHE, and only  
922  
923 383 after longer treatments, able to attain more than 95% of inactivation, both staining  
924  
925 384 percentages were similar. However, in the case of acid-exposed cells, the amount of  
926  
927 385 HPF-stained cells was slightly superior to that of DHE-stained cells.  
928  
929 386 In order to confirm the order of appearance of these phenomena, DHE-HPF and HPF-PI  
930  
931 387 double staining was carried out. Cells were stained simultaneously with the two dyes, and  
932  
933 388 the amount of cells stained in red, in green, and with both colors was estimated. The results  
934  
935 389 are shown in Figure 3. We would like to point out that these experiments were repeated at  
936  
937 390 different treatment intensities for each agent, and the observations were similar (data not  
938  
939  
940  
941  
942  
943  
944



945  
946  
947 391 shown). As shown in Fig 3A, when cells were exposed to heat, the appearance of HPF  
948  
949 392 staining in a particular cell was always accompanied by DHE staining. On the contrary,  
950  
951 393 there was a certain percentage of cells (55%) which presented DHE staining, that did not  
952  
953 394 show HPF staining. On the other hand, every heat-treated cell with a PI-permeabilized  
954  
955 395 membrane showed HPF staining, but a certain percentage of cells (67%) with HPF  
956  
957 396 staining maintained a non permeabilized membrane. For HHP treated cells, results  
958  
959 397 (Fig 3B) indicated an order of cellular events similar to that observed for heat-treated  
960  
961 398 cells.

962  
963  
964 399 Results obtained for PEF treated cells were different (Fig 3C), since a great  
965  
966 400 percentage of cells (73%) with a PI-permeabilized membrane did not show HPF  
967  
968 401 staining. Finally, in acid-treated cells (Fig 3D), it is remarkable that the appearance of  
969  
970 402 increased levels of DHE staining was always accompanied by HPF staining, indicating  
971  
972 403 a different mechanism involved in ROS formation and/or elimination in these cells.  
973  
974 404 For heat, HHP and PEF treated cells, hydroxyl radicals could be formed as a  
975  
976 405 consequence of superoxide radicals presence. According to some authors, under  
977  
978 406 physiological conditions, ROS production takes place in the order  $O_2^{\cdot-} \rightarrow H_2O_2 \rightarrow OH^{\cdot}$   
979  
980 407 (superoxide  $\rightarrow$  hydrogen peroxide  $\rightarrow$  hydroxyl), due to the consecutive addition of one  
981  
982 408 electron to the oxygen molecule (Imlay, 2003; Lushchak, 2011). For acid- treated cells  
983  
984 409 hydroxyl radicals appeared more intensely than in cells treated by the other agents,  
985  
986 410 suggesting a different origin of the oxidative radicals present.

987  
988  
989 411 As a whole view, and taking into account results from Fig 2 and 3, increased levels  
990  
991 412 of ROS and membrane permeabilization were detected in cells treated by the four  
992  
993 413 technologies, therefore the two phenomena could be involved in cell inactivation.  
994  
995 414 However, the relative importance of the two cellular events on cell survival and  
996  
997 415 inactivation seems different. We can hypothesize that increased ROS levels could be  
998  
999  
1000  
1001  
1002  
1003

1004  
1005  
1006 416 the consequence of an extensively damaged cytoplasmic membrane in the case of PEF  
1007  
1008 417 treatment, but not in the case of the other three technologies. Thus, no clear-cut  
1009  
1010 418 relationship between these two phenomena can be established, although the occurrence  
1011  
1012 419 of subtle membrane alterations leading to increased ROS levels, such as for instance  
1013  
1014 420 damages in particular enzymes in the respiratory chain, cannot be ruled out. Besides, in  
1015  
1016 421 the particular case of acid-treated cells, probably additional cellular mechanisms are  
1017  
1018 422 taking place giving rise to an increased level of hydroxyl radicals. For instance, if  
1019  
1020 423 particular enzymes or structures involved in iron homeostasis were more affected by  
1021  
1022 424 acid exposure, increased intracellular Fenton reaction could rise to uncontrolled  
1023  
1024 425 hydroxyl levels inside the cell.  
1025  
1026

#### 1027 426 **Relationship between cell recovery and cellular staining**

1028  
1029 427 Although results obtained so far suggested that increased levels of ROS after  
1030  
1031 428 treatments could be related to cell inactivation in some of the technologies studied, it  
1032  
1033 429 has to be kept in mind that apparent cell inactivation may widely vary depending on  
1034  
1035 430 the recovery conditions (Fig 1, Table 1). Figure 4 represents the percentage of  
1036  
1037 431 inactivated cells, measured as cells unable to grow in TSAYE, in TSAYE-NaCl, and in  
1038  
1039 432 MM-cys, for cells treated with the four technologies. Treatment conditions applied  
1040  
1041 433 were chosen to obtain an inactivation close to 60% for the four technologies,  
1042  
1043 434 measured in standard recovery conditions (TSAYE, aerobiosis). The percentage of  
1044  
1045 435 cells with positive staining with DHE, HPF and PI has also been included in the  
1046  
1047 436 graph for comparison purposes. Data in Fig 4 show that the percentage of cells with  
1048  
1049 437 ROS (DHE staining for heat, HHP and PEF or HPF staining for acid) was coincident  
1050  
1051 438 with loss of viability measured in TSAYE-NaCl, for the four technologies ( $p>0.05$ ).  
1052  
1053 439 These results were also observed for other experimental conditions (data not shown).  
1054  
1055 440 This fact could indicate that cells with increased levels of ROS would present sublethal  
1056  
1057  
1058  
1059  
1060  
1061  
1062

1063  
1064  
1065 441 injuries, able to be repaired by the cellular machinery. The relationship was lost when  
1066  
1067 442 cells were recovered under milder environmental conditions, for instance TSAYE or,  
1068  
1069 443 most notably, minimal medium plus anaerobic atmosphere (MM-cys). Thus, these  
1070  
1071 444 latter conditions could help cells to effectively control ROS levels and to repair their  
1072  
1073 445 damages. Therefore, the role of increased levels of ROS on cell inactivation and  
1074  
1075 446 survival remains unclear, since a certain proportion of cells with increased levels of  
1076  
1077 447 ROS were able to recover and survive under appropriate environmental conditions.  
1078  
1079 448 Whether increased ROS levels arise from unbalances in the electron transport chain  
1080  
1081 449 located in the membrane, as suggested by other authors (Mols and Abee, 2011), or  
1082  
1083 450 from other cellular alterations such as the massive loss of activity of detoxifying  
1084  
1085 451 enzymes, disassembly of intracellular iron-sulfur clusters, or loss of antioxidant  
1086  
1087 452 intracytoplasmic molecules (for instance glutathione), is something that remains to be  
1088  
1089 453 investigated. Also, the exact reason behind the protective effect of MM-cys-  
1090  
1091 454 anaerobiosis is not known. As discussed above, the most plausible explanation is that  
1092  
1093 455 it could be ascribed to the fact that it represents a lower oxidative-stress burden, as  
1094  
1095 456 compared to other recovery conditions. In any case, these results underscore the need  
1096  
1097 457 to optimize recovery media and conditions, in order to more accurately evaluate the  
1098  
1099 458 number of survivors to food processes. From our results it can be concluded that  
1100  
1101 459 complex media under aerobic recovery conditions underestimate the number of  
1102  
1103 460 survivors to all the technologies studied.

1104  
1105 461 A great percentage of heat-, HHP-, and lactic acid-treated cells was unable to grow in  
1106  
1107 462 the presence of NaCl, while maintained impermeability to PI (Fig 4). Only in the  
1108  
1109 463 particular case of PEF, both percentages were coincident, results that are in  
1110  
1111 464 concordance with those previously reported (Cebrián et al., 2016). These results  
1112  
1113 465 indicate that the nature, magnitude and relevance of membrane damage are different  
1114  
1115  
1116  
1117  
1118  
1119  
1120  
1121

1122  
1123  
1124 466 depending on the technology used. We can hypothesize that heat, HHP and acid  
1125  
1126 467 may be either affecting structures other than the membrane itself, but also involved  
1127  
1128 468 in NaCl homeostasis, or, alternatively, may be causing subtle alterations in the  
1129  
1130 469 cytoplasmic membrane, unable to increase permeability to PI, but still relevant to  
1131  
1132 470 NaCl homeostasis.

### 1133 471 **3.3. Protein and DNA damage**

1134  
1135 471 **3.3. Protein and DNA damage**  
1136  
1137 472 In order to obtain a deeper insight into the mechanisms of inactivation of the four  
1138  
1139 473 technologies, we studied the importance of two additional cellular events: protein and  
1140  
1141 474 DNA damage. On the one hand, we checked the inactivation of two mutant strains  
1142  
1143 475 defective either in the chaperone DnaK, involved in refolding of aberrant proteins  
1144  
1145 476 within the cell, or in the RecA protein, responsible for the DNA-repair mechanism  
1146  
1147 477 through homologous recombination (Doyle et al., 2015; Sharma et al., 2013). And on  
1148  
1149 478 the other hand, we directly evaluated the degree of DNA damage, through agarose  
1150  
1151 479 electrophoresis of a fragment amplified from DNA extracted from treated cells,  
1152  
1153 480 respectively (Park and Imlay, 2003).

1154  
1155  
1156 481 Figure 5 shows the difference in Log cycles of inactivation of the mutant strains as  
1157  
1158 482 compared to the parental BW25113. Results showed that the  $\Delta DnaK$  mutant strain  
1159  
1160 483 was particularly sensitive to HHP treatments, suggesting a primary role of protein  
1161  
1162 484 damage and recovery, mainly in HHP inactivation.

1163  
1164  
1165 485 Conversely, the  $\Delta RecA$  mutant strain was more sensitive to heat treatment and to acid  
1166  
1167 486 treatment. In fact its sensitivity to acid treatment was especially notable. Neither of  
1168  
1169 487 the two mutant strains showed more sensitivity than the parental to PEF treatments,  
1170  
1171 488 suggesting that this technology would cause neither DNA nor protein damage in cells.  
1172  
1173 489 From the results in Figure 5 it can be inferred that DNA is a primary cellular target upon  
1174  
1175 490 acid exposure. Fig 6 shows the DNA electrophoresis of an 1860 bp fragment amplified  
1176  
1177  
1178  
1179  
1180

1181  
1182  
1183 491 from DNA extracted from BW25113 cells treated by the four technologies applied at  
1184  
1185 492 equivalent lethality. As it can be observed in the Figure, DNA from acid-exposed cells  
1186  
1187 493 showed poor amplification, in comparison to DNA from native cells or from heat-, HHP-  
1188  
1189 494 and PEF-treated cells. This poor amplification can be interpreted as a consequence of  
1190  
1191 495 extensive damage, and could be possibly related to the increased presence of hydroxyl  
1192  
1193 496 radical (Fig 2, Fig 4), which is recognized as highly toxic for the genetic material  
1194  
1195 497 (Park and Imlay, 2003).

## 1198 498 **Conclusions**

1199  
1200 499 In summary, results show that increased ROS levels are found inside *E. coli* cells after  
1201  
1202 500 all the treatments applied and their appearance is progressive along treatment time,  
1203  
1204 501 despite the different nature of these agents. Only in the particular case of PEF-  
1205  
1206 502 treated cells occurrence of increased ROS level was coincident with permanent  
1207  
1208 503 permeabilization to PI, which can be considered as indicative of seriously  
1209  
1210 504 compromised membranes. On the contrary, for the other three technologies, the  
1211  
1212 505 presence of increased ROS levels occurred well before permeabilization to PI. In cells  
1213  
1214 506 treated by heat, HHP and PEF, DHE staining preceded HPF staining, and only in the  
1215  
1216 507 particular case of acid-treated cells, HPF staining preceded DHE staining, suggesting  
1217  
1218 508 that in these cells, hydroxyl radicals were formed through a different mechanism, and  
1219  
1220 509 possibly played a more relevant role, particularly in relation to DNA damage.

1221  
1222 510 Results obtained in this investigation add new data to help to understand the mode of  
1223  
1224 511 action of food preservation technologies on bacterial cells. This knowledge would help  
1225  
1226 512 in the design of more effective processes.

## 1230 513 **Acknowledgements**

1231  
1232 514 The authors would like to thank the European Regional Development Fund, MINECO-  
1233  
1234 515 CICYT (AGL2012-33522, AGL2015-69565-P), the Department of Innovation Research

1240  
1241  
1242 516 and University of the Aragon Government and European Social Fund (FSE) for the  
1243  
1244 517 support (predoctoral grant M. Marcén, C093/2014).

1246 518 **REFERENCES**

1248  
1249 519 Aertsen A, De Spiegeleer P, Vanoirbeek K, Lavilla M, Michiels CW. 2005. Induction  
1250  
1251 520 of oxidative stress by high hydrostatic pressure in *Escherichia coli*. Appl. Environ.  
1252  
1253 521 Microbiol. 71:2226-2231.

1254  
1255 522 Álvarez, I, Virto R, Raso J, Condón S. 2003. Comparing predicting models for the  
1256  
1257 523 *Escherichia coli* inactivation by pulsed electric fields. Innov. Food Sci. Emerg. Technol.  
1258  
1259 524 4:195-202.

1260  
1261 525 Baatout S, De Boever P, Mergeay M. 2005. Temperature- induced changes in  
1262  
1263 526 bacterial physiology as determined by flow cytometry. Ann. Microbiol. 55:73-80.

1264  
1265 527 Benito A, Ventoura G, Casadei M, Robinson T, Mackey B. 1999. Variation in  
1266  
1267 528 resistance of natural isolates of *Escherichia coli* O157 to high hydrostatic pressure, mild  
1268  
1269 529 heat, and other stresses. Appl. Environ. Microbiol. 65:1564-1569.

1270  
1271  
1272 530 Cebrián G, Sagarzazu N, Pagan R, Condón S, Mañas P. 2007. Heat and pulsed electric  
1273  
1274 531 field resistance of pigmented and non-pigmented enterotoxigenic strains of  
1275  
1276 532 *Staphylococcus aureus* in exponential and stationary phase of growth. Int. J. Food  
1277  
1278 533 Microbiol. 118:304-311.

1280 534 Cebrián G., Sagarzazu N., Pagán R., Condón S., Mañas P. 2010. Development of stress  
1281  
1282 535 resistance in *Staphylococcus aureus* after exposure to sublethal environmental  
1283  
1284 536 conditions. Int. J. Food Microbiol. 140:26-33.

1285  
1286  
1287 537 Cebrián G, Condón S, Mañas P. 2016. Influence of growth and treatment temperature  
1288  
1289 538 on *Staphylococcus aureus* resistance to pulsed electric fields. Relationship with  
1290  
1291 539 membrane fluidity. Innov. Food Sci. Emerg. Technol. 37:161-169.

1292  
1293 540 De Spiegeleer P, Sermon J, Lietaert A, Aertsen A, Michiels C. 2004. Source of

1299  
1300  
1301 541 tryptone in growth medium affects oxidative stress resistance in *Escherichia coli*. J.  
1302  
1303 542 Appl. Microbiol. 97:124-133.  
1304  
1305 543 Doyle SM, Shastry S, Kravats AN, Shih YH, Miot M, Hoskins JR, Stan G, Wickner S.  
1306  
1307 544 2015. Interplay between *E. coli* DnaK, ClpB and GepE during protein disaggregation. J.  
1308  
1309 545 Mol. Biol. 427:312-327.  
1310  
1311  
1312 546 Geeraerd A, Herremans C, Van Impe J. 2000. Structural model requirements to  
1313  
1314 547 describe microbial inactivation during a mild heat treatment. Int. J. Food Microbiol.  
1315  
1316 548 59:185-209.  
1317  
1318 549 Geeraerd A, Valdramidis V, Van Impe J. 2005. GInaFiT, a freeware tool to assess  
1319  
1320 550 non-log-linear microbial survivor curves. Int. J. Food Microbiol. 102:95-105.  
1321  
1322 551 Gerhardt P, Murray RGE, Wood WA, Krieg NR. 1994. Methods for General and  
1323  
1324 552 Molecular Bacteriology, vol 1325. American Society for Microbiology, Washington,  
1325  
1326 553 DC.  
1327  
1328  
1329 554 Gomes A, Fernandes E, Lima JL. 2005. Fluorescence probes used for detection of  
1330  
1331 555 reactive oxygen species. J. Biochem. Biophys. Meth. 65:45-80.  
1332  
1333 556 Gusarov I, Nudler E. 2005. NO-mediated cytoprotection: instant adaptation to  
1334  
1335 557 oxidative stress in bacteria. Proceedings of the National Academy of Science USA  
1336  
1337 558 102:13855-13860.  
1338  
1339 559 Imlay JA. 2003. Pathways of oxidative damage. Ann. Rev. Microbiol. 57:395-418.  
1340  
1341 560 Imlay JA. 2013. The molecular mechanisms and physiological  
1342  
1343 561 consequences of oxidative stress: lessons from a model bacterium. Nat. Rev. Microbiol.  
1344  
1345 562 11:443.  
1346  
1347  
1348 563 Klotz B, Mañas P, Mackey BM. 2010. The relationship between membrane damage,  
1349  
1350 564 release of protein and loss of viability in *Escherichia coli* exposed to high  
1351  
1352 565 hydrostatic pressure. Int. J. Food Microbiol. 137:214-220.  
1353  
1354  
1355  
1356  
1357

- 1358  
1359  
1360 566 Lado BH, Yousef AE. 2002. Alternative food-preservation technologies: efficacy and  
1361  
1362 567 mechanisms. *Microbes Infect.* 4:433-440.  
1363  
1364 568 Lou Y, Yousef AE. 1997. Adaptation to sublethal environmental stresses protects  
1365  
1366 569 *Listeria monocytogenes* against lethal preservation factors. *Appl. Environ.*  
1367  
1368 570 *Microbiol.* 63:1252-1255.  
1370  
1371 571 Lushchak VI. 2011. Adaptive response to oxidative stress: bacteria, fungi, plants and  
1372  
1373 572 animals. *Comp. Biochem. Physiol. C Toxicol. Pharmacol.* 153:175-190.  
1374  
1375 573 Mackey B. 2000. Injured bacteria, p 315-341. *In* Lund B, Baird-Parker, TC., Gould,  
1376  
1377 574 GW. Eds. (ed), *The microbiological safety and quality of food*, vol 1. Springer.  
1378  
1379 575 Mackey BM, Mañas P. 2008. Inactivation of *Escherichia coli* by high pressure, p 53-  
1380  
1381 576 85, *High-pressure microbiology*. American Society of Microbiology.  
1382  
1383 577 Malone AS, Chung YK, Yousef AE. 2006. Genes of *Escherichia coli* O157: H7 that  
1384  
1385 578 are involved in high-pressure resistance. *Appl. Environ. Microbiol.* 72:2661-2671  
1386  
1387 579 Mañas P, Pagán R. 2005. Microbial inactivation by new technologies of food  
1388  
1389 580 preservation. *J. Appl. Microbiol.* 98:1387- 1399.  
1390  
1391 581 Marcén M, Ruiz V, Serrano MJ, Condón S, Mañas P. 2017. Oxidative stress in *E. coli*  
1392  
1393 582 cells upon exposure to heat treatments. *Int. J. Food Microbiol.* 241:198-205.  
1394  
1395 583 Miles CA. 2006. Relating cell killing to inactivation of critical components. *Appl.*  
1396  
1397 584 *Environ. Microbiol.* 72:914-917.  
1398  
1399 585 Mols M, Pier I, Zwietering MH, Abee T. 2009. The impact of oxygen availability on  
1400  
1401 586 stress survival and radical formation of *Bacillus cereus*. *Int. J. Food Microbiol.* 135:303-  
1402  
1403 587 311.  
1404  
1405 588 Mols M, Van Kranenburg R, Van Melis CC, Moezelaar R, Abee T. 2010. Analysis of  
1406  
1407 589 acid-stressed *Bacillus cereus* reveals a major oxidative response and inactivation-  
1408  
1409 590 associated radical formation. *Environ. Microbiol.* 12:873-885.  
1410  
1411  
1412  
1413  
1414  
1415  
1416



- 1417  
1418  
1419 591 Mols M, Abee T. 2011. Primary and secondary oxidative stress in *Bacillus*.  
1420  
1421 592 Environ. Microbiol. 13:1387-1394.  
1422  
1423 593 Pakhomova ON, Khorokhorina VA, Bowman AM, Rodaitė-Riševičienė R, Saulis G,  
1424  
1425 594 Xiao S, Pakhomov AG. 2012. Oxidative effects of nanosecond pulsed electric field  
1426  
1427 595 exposure in cells and cell-free media. Arch. Biochem. Biophys. 527:55-64.  
1428  
1429 596 Park S, Imlay JA. 2003. High levels of intracellular cysteine promote oxidative DNA  
1430  
1431 597 damage by driving the fenton reaction. Bacteriol. 185:1942-1950.  
1432  
1433 598 Patsoukis N, Papapostolou I, Georgiou CD. 2005. Interference of non-specific  
1434  
1435 599 peroxidases in the fluorescence detection of superoxide radical by hydroethidine  
1436  
1437 600 oxidation: a new assay for H<sub>2</sub>O<sub>2</sub>. Anal. Bioanal. Chem. 381:1065-1072.  
1438  
1439 601 Ramos SJ., Chiquirrín M., García S., Condón S., Pérez MD. 2015. Effect of high  
1440  
1441 602 pressure treatment on inactivation of vegetative pathogens and on denaturation of whey  
1442  
1443 603 proteins in different media. LWT-Food Sci. Technol. 63:732-738.  
1444  
1445 604 Richard H, Foster JW. 2004. *Escherichia coli* glutamate-and arginine-dependent acid  
1446  
1447 605 resistance systems increase internal pH and reverse transmembrane potential. J.  
1448  
1449 606 Bacteriol. 186:6032-6041.  
1450  
1451 607 Saldaña G, Puértolas E, Álvarez I, Meneses N, Knorr D, Raso J. 2010. Evaluation  
1452  
1453 608 of a static treatment chamber to investigate kinetics of microbial inactivation by  
1454  
1455 609 pulsed electric fields at different temperatures at quasi-isothermal conditions. J.  
1456  
1457 610 Food Eng. 100:349-356.  
1458  
1459 611 San Martin M, Barbosa-Cánovas G, Swanson B. 2002. Food processing by high  
1460  
1461 612 hydrostatic pressure. Crit. Rev. Food Sci. and Nutr. 42:627-645.  
1462  
1463 613 Sharma V, Sakai Y, Smythe KA, Yokobayashi Y. 2013. Knockdown of *recA* gene  
1464  
1465 614 expression by artificial small RNAs in *Escherichia coli*. Biochem. Biophys. Res.  
1466  
1467 615 Commun. 430:256-259.  
1468  
1469  
1470  
1471  
1472  
1473  
1474  
1475

1476  
1477  
1478  
1479  
1480  
1481  
1482  
1483  
1484  
1485  
1486  
1487  
1488  
1489  
1490  
1491  
1492  
1493  
1494  
1495  
1496  
1497  
1498  
1499  
1500  
1501  
1502  
1503  
1504  
1505  
1506  
1507  
1508  
1509  
1510  
1511  
1512  
1513  
1514  
1515  
1516  
1517  
1518  
1519  
1520  
1521  
1522  
1523  
1524  
1525  
1526  
1527  
1528  
1529  
1530  
1531  
1532  
1533  
1534

616 Stanier RY, Ingraham JL, Wheelis ML, Painter PR. 1992. Microbiología, 2nd ed.  
617 Reverté S.A, Barcelona.  
618 Suh JH, Knabel SJ. 2000. Comparison of different reducing agents for enhanced  
619 detection of heat-injured *Listeria monocytogenes*. J. Food Prot. 63:1058-1063.  
620 Van de Guchte M, Serror P, Chervaux C, Smokvina T, Ehrlich SD, Maguin E. 2002.  
621 Stress responses in lactic acid bacteria. Antonie Van Leeuwenhoek 82:187-216.  
622 Wuytack EY, Phuong LDT, Aertsen A, Reyns K, Opstal I, Diels A, Michiels C. 2003.  
623 Comparison of sublethal injury induced in *Salmonella enteric* serovar Typhimurium by  
624 heat and by different nonthermal treatments. J. Food Prot. 66:31-37.  
625 Zielonka, J., Kalyanaraman, B., 2010. Hydroethidine-and MitoSOX-derived red  
626 fluorescence is not a reliable indicator of intracellular superoxide formation: another  
627 inconvenient truth. Free Radic. Biol. Med. 48(8), 983-1001.

628

1535  
1536  
1537 **Table 1.** Resistance parameters ( $S_i$ ,  $k_{max}$ ,  $N_{res}$ ,  $D$  and  $2D$ ) obtained from the fitting of  
1538  
1539 Geeraerd model, and area under the curve (AUC) corresponding to survival curves of *E.*  
1540  
1541  
1542 *coli* treated by different agents (heat, HHP, PEF and acidity).  
1543

	Heat		
	TSAYE	TSAYE + NaCl	MM-cys
$S_i$	1.41 ± 0.34	0.80 ± 0.13	2.01 ± 0.14
$k_{max}$	3.40 ± 0.48	7.43 ± 0.79	1.84 ± 0.15
$D$	0.68 ± 0.09	0.31 ± 0.03	1.26 ± 0.20
$2D$	2.78 ± 0.16	1.43 ± 0.12	4.52 ± 0.10
RMSE	0.137	0.434	0.125
$R^2$	0.97	0.98	0.98
AUC	1.79	5.07	0.596
	HHP		
	TSAYE	TSAYE + NaCl	MM-cys
$S_i$	2.90 ± 0.26	0.21 ± 0.19	6.52 ± 1.88
$k_{max}$	0.57 ± 0.02	0.81 ± 0.03	0.17 ± 0.02
$D$	4.04 ± 0.15	2.84 ± 0.13	13.37 ± 1.96
$2D$	10.98 ± 0.22	5.90 ± 0.20	33.27 ± 2.04
RMSE	0.058	0.070	0.058
$R^2$	0.99	0.99	0.99
AUC	9.08	19.5	2.55
	PEF		
	TSAYE	TSAYE + NaCl	MM-cys
$k_{max}$	0.03 ± 0.01	0.05 ± 0.01	0.02 ± 0.00
$N_{res}$	-2.96 ± 0.29	-3.06 ± 0.12	
$D$	76.25 ± 2.50	49.82 ± 2.24	139.16 ± 2.37
$2D$	152.51 ± 3.31	99.64 ± 4.27	278.33 ± 4.74
RMSE	0.204	0.224	0.149
$R^2$	0.97	0.98	0.97
AUC	161	243	84.5
	Acidity		
	TSAYE	TSAYE + NaCl	MM-cys
$S_i$	65.10 ± 7.97	5.67 ± 1.51	
$k_{max}$	0.09 ± 0.02	0.13 ± 0.01	
$D$	24.32 ± 2.53	17.64 ± 0.94	
$2D$	113.75 ± 3.33	40.96 ± 2.44	
RMSE	0.086	0.037	
$R^2$	0.97	0.99	
AUC	68.15	307.6	

1582  
1583  
1584  
1585  
1586  
1587  
1588  
1589  
1590  
1591  
1592  
1593

632  
633  $S_i$  (shoulder length): min;  $k_{max}$  (inactivation rate): 1/min (heat, HHP and acidity) and 1/ $\mu$ s (PEF);  $N_{res}$  (residual population density):  
634 (Log<sub>10</sub> CFU/mL);  $D$  (decimal reduction time value) and  $2D$  (time for inactivation of the first two Log cycles): min (heat, HHP and  
635 acidity) and  $\mu$ s (PEF); AUC (Area Under the Curve): min x log<sub>10</sub> CFU (heat, HHP and acidity) and  $\mu$ s x log<sub>10</sub> CFU (PEF).  
636 Goodness of fit is indicated by maximum RMSE (root mean squared error) and minimum  $R^2$  (determination coefficient).  
637

1594  
1595  
1596 641 **FIGURE CAPTIONS**  
1597

1598 642

1600 643 **Fig. 1.** Survival curves of *E. coli* BW25113 obtained in TSAYE (●), TSAYE-NaCl (■)  
1601  
1602 644 and MM-cys (▲) after treating cells by heat (58°C) (A), HHP (300 MPa) (B), PEF (20  
1603  
1604 645 kV/cm) (C) and acidity (pH 3.0) (D).  
1606

1607 646

1608 647 **Fig. 2.** Percentage of inactivated (●) and stained cells with DHE (○), HPF (Δ) and PI  
1609  
1610 648 (□) of *E. coli* BW25113 along time for each treatment applied: heat (58°C) (A), HHP  
1611  
1612 649 (300 MPa) (B), PEF (20 kV/cm) (C) and acidity (pH 3.0) (D).  
1614

1615 650

1617 651 **Fig. 3.** Single (DHE, HPF, PI) and double staining (DHE-HPF and HPF-PI) of *E. coli*  
1618  
1619 652 cells treated by heat (58°C/1 min) (A), HHP (300 MPa/8 min) (B), PEF (20 kV/cm/30  
1620  
1621 653 μs) and acidity (pH 3.0/30 min) (D).  
1622

1623 654

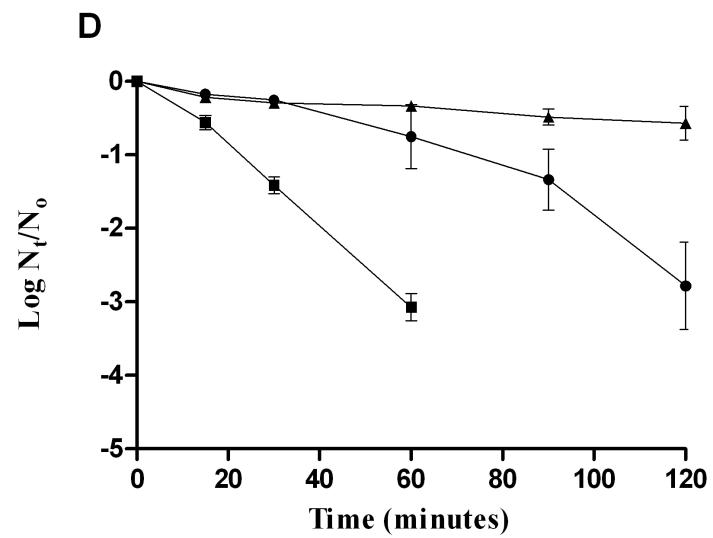
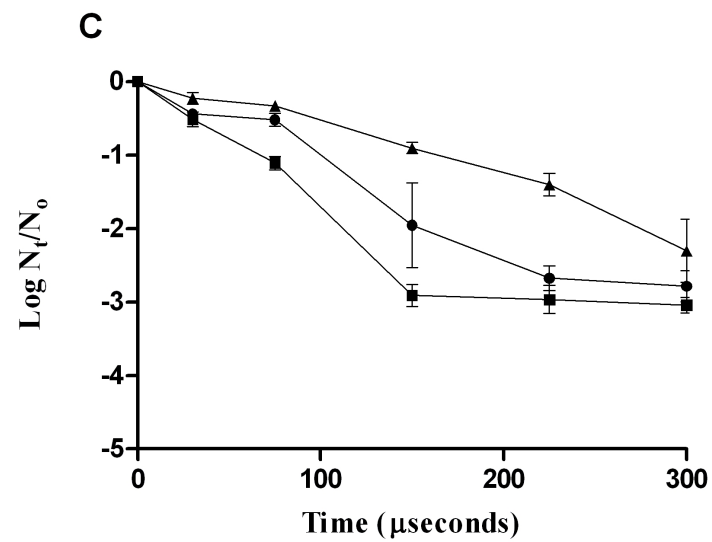
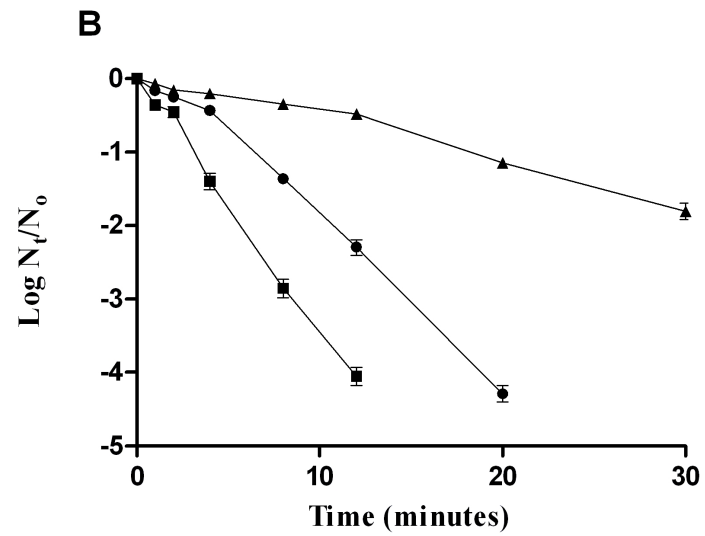
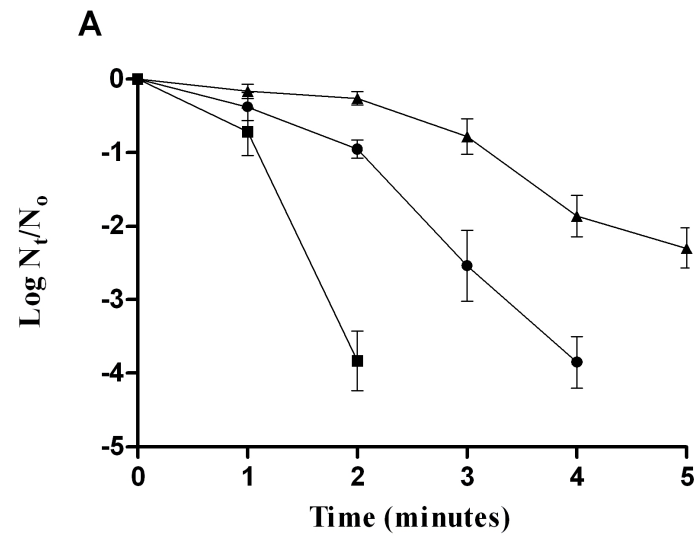
1625 655 **Fig. 4.** Comparison between the percentage of inactivated cells recovered in TSAYE,  
1626  
1627 656 TSAYE-NaCl and MM-cys and the percentage of cells stained with DHE, HPF and PI  
1628  
1629 657 after treating *E. coli* BW25113 with different technologies: heat (58°C/1 min) (white  
1630  
1631 658 bars), HHP (300 MPa/4 min) (soft grey bars), PEF (20 kV/cm/30 μs) (dark grey bars)  
1632  
1633 659 and acidity (pH 3.0/ 60min) (black bars).  
1635

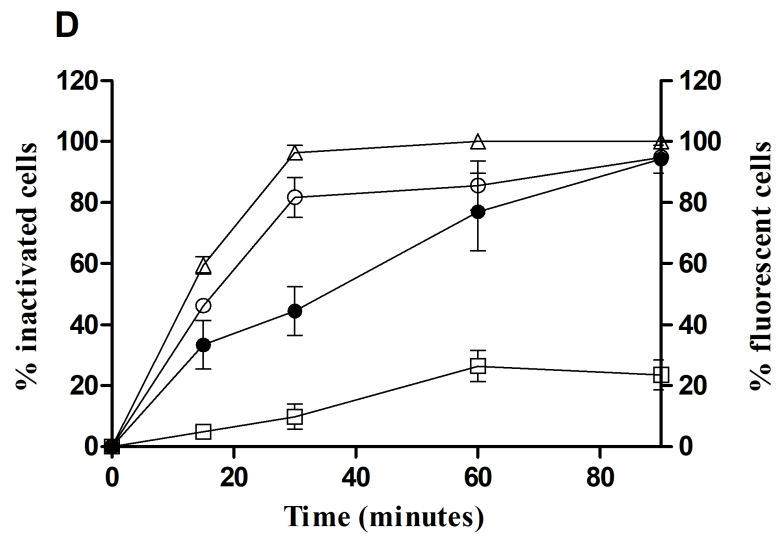
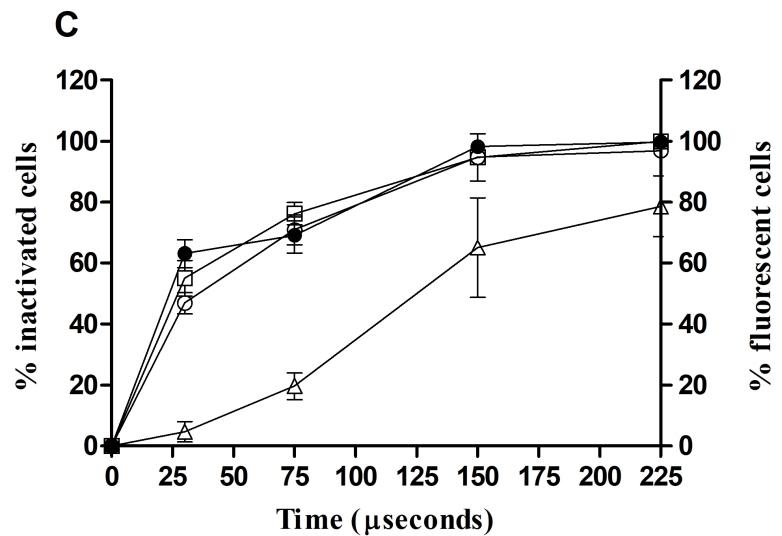
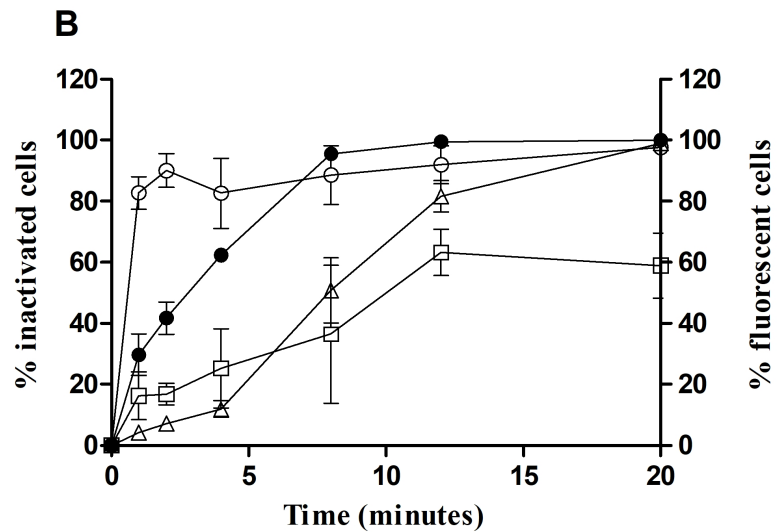
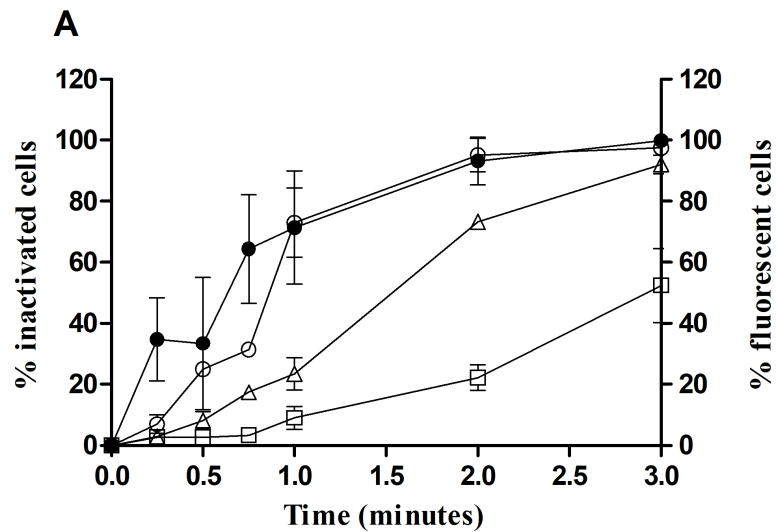
1636 660

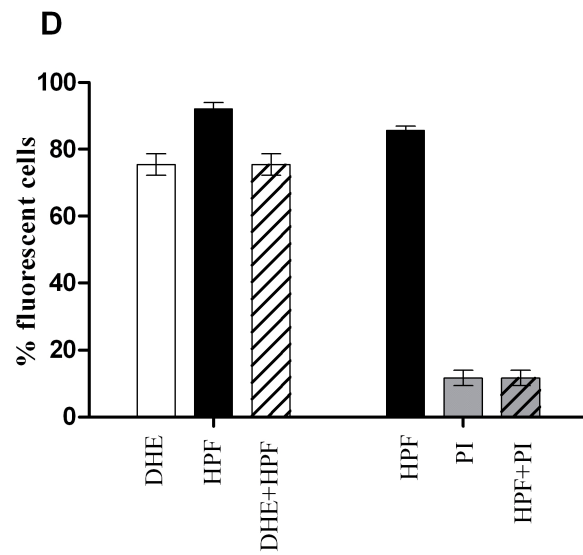
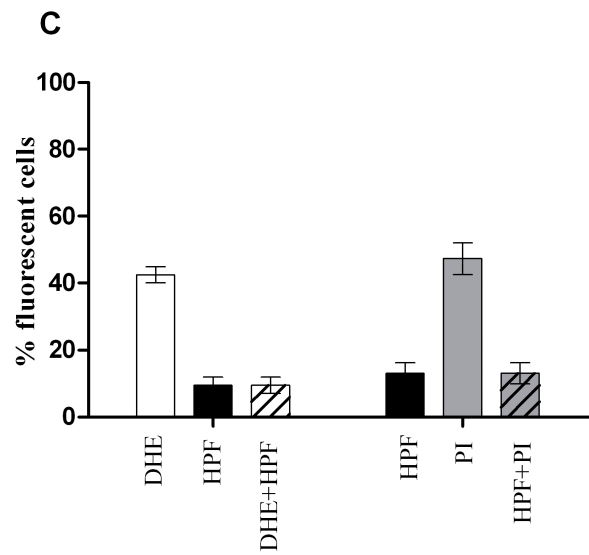
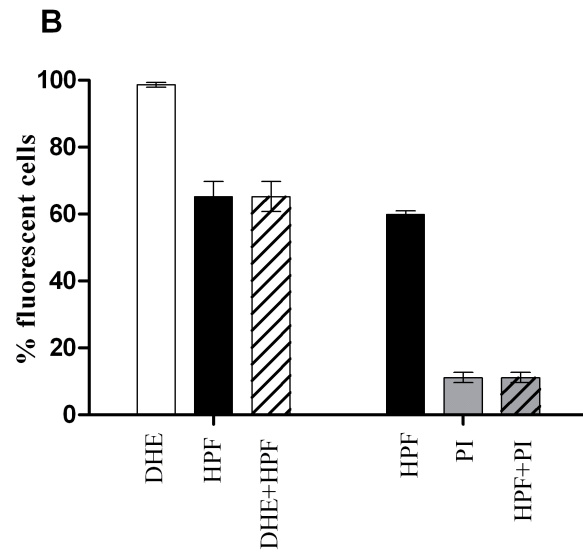
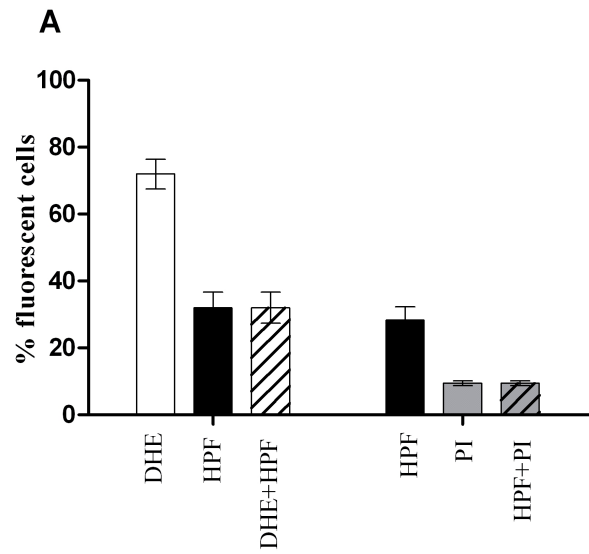
1638 661 **Fig. 5.** Difference in Log cycles of inactivation of the mutant strains  $\Delta DnaK$  (grey bars)  
1639  
1640 662 and  $\Delta RecA$  (black bars) in comparison to the parental strain for the treatments with each  
1641  
1642 663 technology: heat (58°C/3 min), HHP (300 MPa/8 min), PEF (20 kV/cm/225 μs) and  
1643  
1644 664 acidity (pH 3.0/60 min). Cells were recovered in MM-cys.  
1645

1646 665  
1647  
1648  
1649  
1650  
1651  
1652

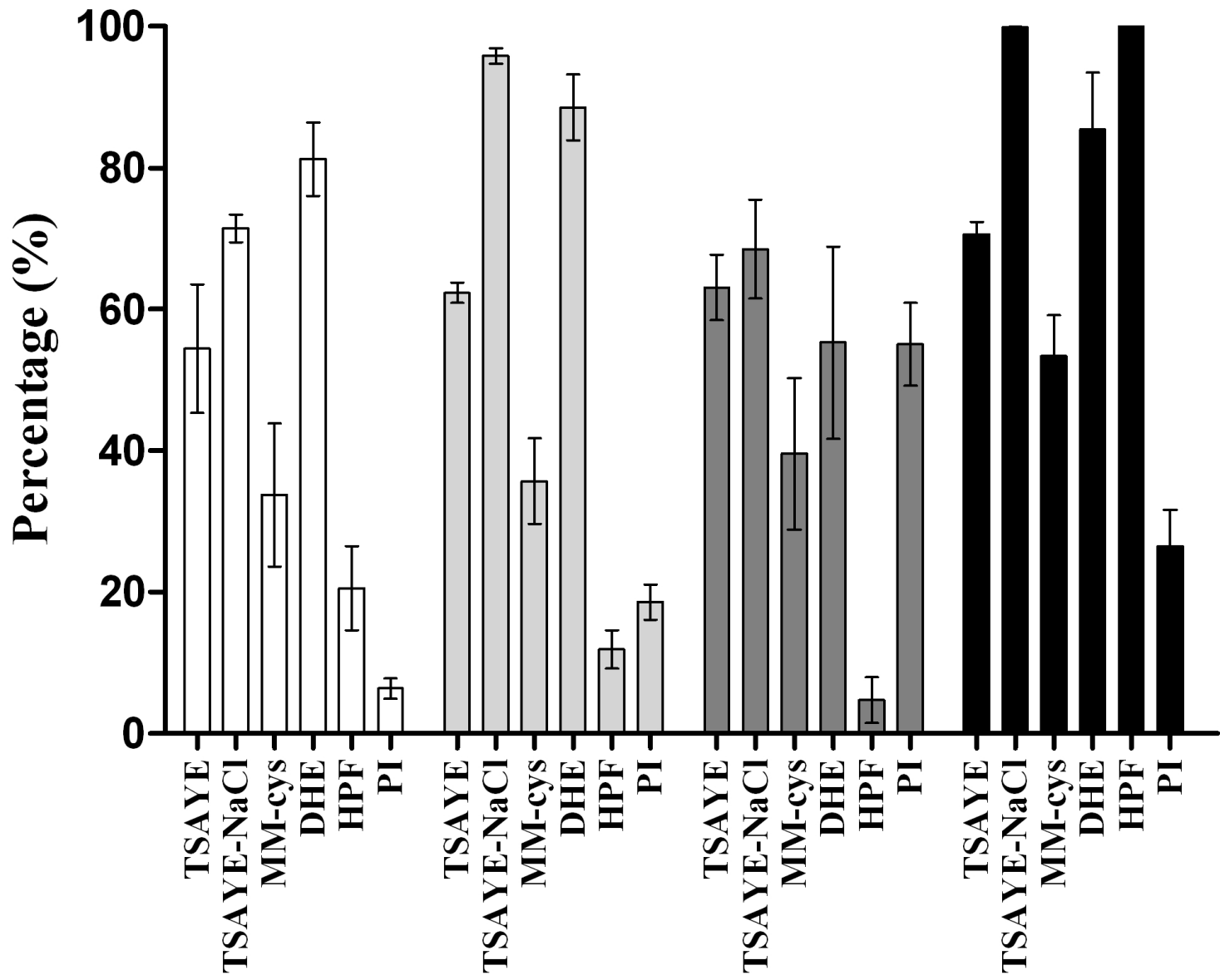
1653  
1654  
1655 666 **Fig. 6.** DNA electrophoresis of an 1860pb fragment amplified from DNA extracted  
1656  
1657 667 from *E. coli* BW25113 native cells and cells treated by heat (58°C/3 min), HHP (300  
1658  
1659 668 MPa/8 min), PEF (20 kV/cm/225 µs) and acidity (pH 3.0/60 min) at equivalent lethality  
1660  
1661 669 (1.7±0.3 log cycles). Samples appear in the following order from left to right: DNA  
1662  
1663 670 ladder, native cells, heat, HHP, PEF and acidity.  
1664  
1665  
1666  
1667  
1668  
1669  
1670  
1671  
1672  
1673  
1674  
1675  
1676  
1677  
1678  
1679  
1680  
1681  
1682  
1683  
1684  
1685  
1686  
1687  
1688  
1689  
1690  
1691  
1692  
1693  
1694  
1695  
1696  
1697  
1698  
1699  
1700  
1701  
1702  
1703  
1704  
1705  
1706  
1707  
1708  
1709  
1710  
1711

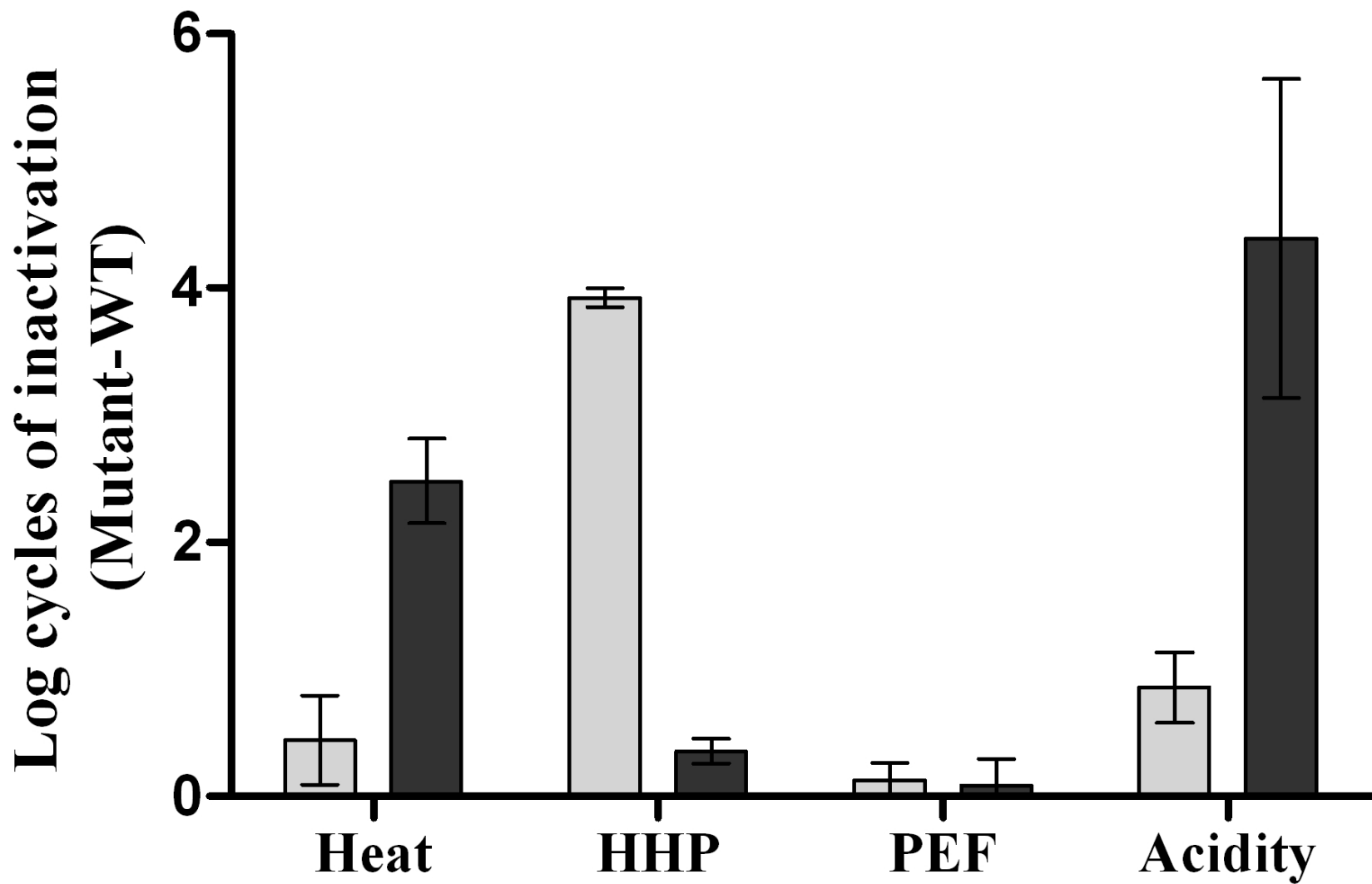












6000  
3000  
2000  
1500  
1000  
250

